A Distinctive Structural Twist in the Aminoimidazole Alkaloids from a Calcareous Marine Sponge: Isolation and Characterization of Leucosolenamines A and B

Paul Ralifo,[†] Karen Tenney,[†] Frederick A. Valeriote,[‡] and Phillip Crews*[,†]

Department of Chemistry and Biochemistry and Institute of Marine Sciences, University of California, Santa Cruz, California 95064, and Division of Hematology and Oncology, Josephine Ford Cancer Center, Detroit, Michigan 48202

Received September 19, 2006

Bioassay-guided fractionation of Papua New Guinea collections of *Leucosolenia* sp. resulted in the isolation of the novel compounds leucosolenamines A (**5**) and B (**6**) and the known compound thymidine (**7**). Compound **5** contains a 2-aminoimidazole core substituted at C-4 and C-5 by an *N,N*-dimethyl-5,6-diaminopyrimidine-2,4-dione and a benzyl group, respectively. Compound **6** retains the same core structure; however C-4 is substituted by a 5,6-diamino-1,3-dimethyl-4-(methylimino)-3,4-dihydropyrimidin-2(1*H*)-one moiety. This substitution pattern is unique and has never been observed in calcareous imidazole alkaloid chemistry. Leucosolenamine A (**5**) was mildly cytotoxic against the murine colon adenocarcinoma C-38 cell line.

The sustained position of marine sponges as a source of structurally diverse and biologically active natural products was emphasized in a recent review article covering the 2003 literature.[1] Complex sponge natural products have also been the basis for the development of several clinical leads.[2] At the top of the list are natural products containing multiple chiral centers such as the bengamides,[3] fijianolides,[4] the halichondrin analogue E7389,[5] and the discodermolides[6] or sponge metabolites with exotic functionality, as in the psammaplins.[7] The research described in this paper began with the goal of adding additional unique structures to the rapidly growing list of sponge-derived alkaloids. In this regard, the Calcarea class of sponges is now recognized as a reliable source of richly bioactive metabolites possessing a 2-aminoimidazole[8] core that is often further substituted at the C-4 and C-5 positions.[9] The range of substitution patterns observed to date at these positions include (a) benzyl side chains, (b) oxo groups at C-4, and (c) annulation by five- or six-membered rings. The structures of naamine C (**1**),[10] leucettamine B (**2**),[11] spirocalcaridine A (**3**),[8c] and 2-amino-2-deoxykealiiquinone (**4**)[12] provide illustrations of these structural features.

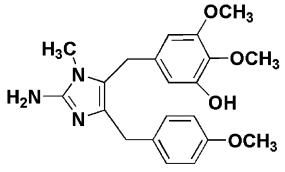

naamine C (**1**)

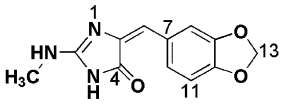

leucettamine B (**2**)

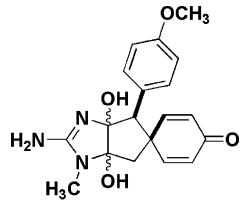

(-)-spirocalcaridine A (**3**)

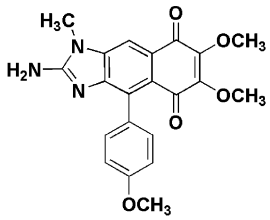

2-amino-2-deoxy-kealiiquinone (**4**)

Investigations to date of Calcarea sponges have been restricted to the genera *Leucetta* (syn. *Pericharax*) and *Clathrina* (both of the order Clathrinida, family Leucettidae). Yet, in view of the rich chemistry discovered, it is surprising that very little chemical work has been conducted on other members of this taxonomic class comprised of sponges in five orders spanning more than 75 genera.[13] The major impediment to further studies of this group is that they appear to be less abundant and poorly described in comparison to the class Demospongiae. During recent expeditions to Papua New Guinea (PNG), specimens of the genus *Leucosolenia* (order Leucosolenida, family Lecucosoleniidae) were obtained and became high priority for further investigation because the crude MeOH extract showed positive activity in our primary screen for in vitro solid tumor selectivity.[14] Disclosed below are the results of this study culminating in the characterization two new compounds, leucosolenamines A (**5**) and B (**6**), possessing a 2-amino imidazole core substituted at C-4 and C-5, and the isolation of thymidine (**7**).

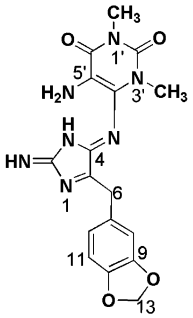

leucosolenamine A (**5**)

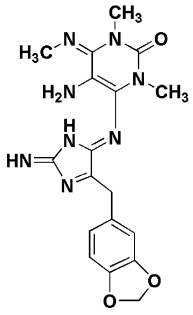

leucosolenamine B (**6**)

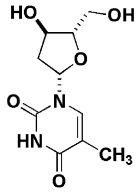

thymidine (**7**)

Results and Discussion

The PNG sponge *Leucosolenia* sp. (coll. no. 03528) yielded three extracts using an accelerated solvent extraction process. The methanol-soluble fraction, coded XFM, had selective bioactivity (for murine adenocarcinoma C-38 cell line) in the disk diffusion solid tumor whole cell assay with an inhibitory zone differential of 9 mm between murine C-38 and CFU-GM cells at 180 μg per disk.[14] Because of this selective bioactivity, the MeOH fraction was subjected to HPLC purification to afford five fractions (Figure S2). Fraction 3 was pure leucosolenamine A (**5**) (5.6 mg) with an *m*/*z* of 384.2 $[M + H]^+$ (ESI-TOF) and exhibited inhibition zones of 10.5 mm (at 180 μg per disk) against murine colon 38 (vs 0 mm against CFU-GM). Fraction 1 (coded XFMP1) was also active and showed an inhibition zone of 21 mm (at 180 μg per disk) against C-38 and was further purified by HPLC to yield thymidine (**7**) (12.2 mg). Additional samples of *Leucosolenia* sp. (coll. no. 05413 and

* Corresponding author. Tel: 831-459-2603. Fax: 831-459-2935. E-mail: phil@chemistry.ucsc.edu.
[†] University of California, Santa Cruz.
[‡] Josephine Ford Cancer Center.

10.1021/np060462b CCC: $37.00
Published on Web 12/22/2006

Table 1. NMR Data of Leucosolenamine (**5**)[a] and Leucettamine B (**2**)[b]

	5 (in DMSO-d_6)			**2** (in Me_2CO-d_6)	
C#	δ_C	δ_H mult. *J* (Hz), int.	gHMBC	δ_C	δ_H mult. *J* (Hz), int.
2	160.1			160.2	
4	148.0			170.5	
5	158.0			140.4	
6	38.1	4.05 s, 2H	C-4, C-5, C-7, C-8, C-12	114.6	6.42 s, 1H
7	133.2			131.7	
8	109.7	6.97 d, *J* 1.5, 1H	C-6, C-9, C-10, C-12	110.8	8.04 d, *J* 1.6, 1H
9	146.8			148.6	
10	145.3			148.1	
11	107.8	6.73 d, *J* 8.0, 1H	C-9, C-7	108.8	6.82 d, *J* 8.1, 1H
12	121.9	6.79 dd, *J* 1.5, 8.0, 1H	C-6, C-8, C-10	126.3	7.33 dd, *J* 1.6, 8.1, 1H
13	100.5	5.90 s, 2H	C-9, C-10	102.0	6.01 s, 2H
2′	150.8				
4′	146.3				
5′	113.7				
6′	159.5				
CH_3-*N*-1′	28.0	3.24 s, 3H	C-2′, C-6′		
CH_3-*N*-3′	28.8	3.39 s, 3H	C-2′, C-4′		

[a] Measured at 500 MHz (^{1}H) and 125 MHz (^{13}C). [b] Ref 11.

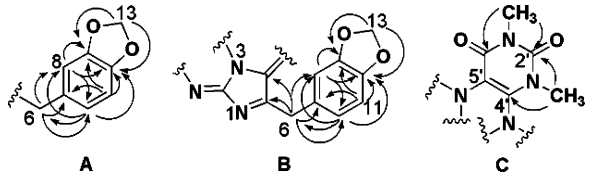

Figure 1. Substructures with observed gHMBC correlations of **5**.

06231) were also examined to isolate more of **5**. To our delight, these two collections (vide infra) yielded **5** accompanied by a new analogue, leucosolenamine B (**6**).

The structure elucidation of **5** began by dereplicating against known sponge-derived metabolites, and the only literature match, naamine C (**1**)[10] [$C_{21}H_{25}N_3O_4$, 383 amu], was confidently ruled out from the atom count assessed by NMR. A partial formula for **5** of $C_{17}H_{13}O_2N_3$ was supported by (a) the ^{13}C and DEPT NMR data (Table 1) showing 10 quaternary, three methine, two methylene, and two methyl carbons, (b) the δ_C 160.1 characteristic of a guanidine residue of a 2-amino imidazole group, and (c) the δ_C/δ_H 100.5/5.90 (s, 2H's) indicative of the 1,3 dioxolane ring as seen in leucettamine B (**2**).[11]

Successive sets of high-resolution mass spectrometry data were needed to finalize the molecular formula of **5** as $C_{17}H_{17}O_4N_7$. The HRESI-TOFMS gave an $[M + H]^+$ *m/z* of 384.1776; however, more accurate data were obtained later by the FTICRMS[15] $[M + H]^+$ *m/z* of 384.14161. Initially we considered three formulas based on the ESI-TOF peak as follows: (i) $C_{17}H_{22}O_2N_9$ (Δ12 mmu vs calc), (ii) $C_{17}H_{18}O_4N_7$ (Δ36 mmu vs calc), and (iii) $C_{17}H_{14}O_6N_5$ (Δ83 mmu vs calc). At this point in the analysis (i) was favored; however, the ultrahigh-resolution data indicated the best match was with (ii) because of the following pattern of Δ mmu vs calc: (ii) = 0.04, (iii) = 47.2, and (i) = 48.0. Comparing the final formula to the partial formula derived by NMR as noted above indicated that four heteroatom-attached hydrogens were present and an unsaturation number of 13 was required.

The ^{1}H NMR spectrum of **5** (Figure S4) was not information rich, as it showed just seven types of signals. As a confounding complication, none of the four heteroatom protons were visible by ^{1}H NMR using a variety of solvents. There was an ABX spin system for a 1,2,4-trisubstituted benzene ring identified by a double doublet at δ 6.79 (J = 1.5, 8.0 Hz), a doublet at δ 6.97 (J = 1.5 Hz), and a doublet at δ 6.73 (J = 8.0 Hz). This diagnostic spin system, the methylene singlet at δ 4.05, and the additional methylene singlet (δ 5.90) noted above justified substructure **A** (Figure 1). This array was confirmed by gHMBC correlations illustrated in Figure 1 and further justified by comparison of NMR properties of **A** to the parallel peaks of leucettamine B (**2**).[11] The remaining observed protons were identified as *N*-methyl singlets at δ 3.39 and 3.24 that flanked the intense water peak.

The process of accounting for the seven nitrogens and four hetero-attached protons of **5** began with the linking of substructure **A** to a 2*N*-imidazole ring, resulting in substructure **B**. This proposal was initially envisioned in order to account for the extraordinarily low field shift of the aliphatic benzylic hydrogens (δ 4.05). The gHMBC correlations shown in Figure 1 were in full agreement with attachment of this heterocyclic ring to C-6. A side-by-side comparison of the ^{13}C and ^{1}H NMR data of leucosolenamine (**5**) and leucettamine B (**2**) at atom numbers 2 and 7−13 provided expected similarities, as shown in Table 1, which further documented their congruent structural features. The obvious differences between these two compounds were also reflected in differing shifts at atom numbers 4−6.

The extremely difficult final task involved assembling one or more substructures to explain the remaining unaccounted atoms of $C_6H_{10}O_2N_4$. The ^{13}C NMR signals to be rationalized consisted of four quaternary carbons (δ_C 159.5, 150.8, 146.3, and 113.7). Also needing a specific assignment were the two *N*-methyls ($\delta_{C/H}$ 28.8/3.39 and 28.0/3.24), noted above. A 5,6-dinitrogen-substituted uracil with *N*-methylation at both ring nitrogens, as shown in substructure **C** of Figure 1, was envisioned and was consistent with these data. Validation of this proposal was partially provided by gHMBC correlations, outlined in Figure 1, from $H_{CH3-N-1'}$ (δ_H 3.24) to C-2′ (δ_C 150.8) and to C-6′ (δ_C 159.5) and from $H_{CH3-N-3'}$ (δ_H 3.39) to C-2′ (δ_C 150.8) and to C-4′ (δ_C 146.3).

The process of merging structures **B** and **C** was not straightforward because, as noted above, all attempts to visualize the four *N*H ^{1}H NMR resonances were unsuccessful. To summarize the constraints established above, there were three bridging atom sites in **B** and two in **C**, resulting in a total of six possible working structures, shown in Figure 2. These structures could be divided into two sets on the basis of the presence of an NH_2 group at C-5′ or at C-4′, consisting of **I**−**III** and **IV**−**VI**, respectively. Two structures, **I** and **IV**, of Figure 2, follow the substitution pattern seen in the naamidines[16] and pyronaamidines,[17] as they retain the commonly observed 2-aminoimidazole ring. However one significant change includes a pyrimidinedione moiety attached to the exocyclic nitrogen and the *N*-substitution at C-4 is without biosynthetic precedent. The same unprecedented situation, *N*-substitution at C-4, holds for all other structures (**II**, **III**, **V**, and **VI**). Attempts to distinguish among these six possibilities aided by NOE data were unsuccessful, as no correlations were observed between the *N*-Me groups of substructure **C** and the sp^3 and sp^2

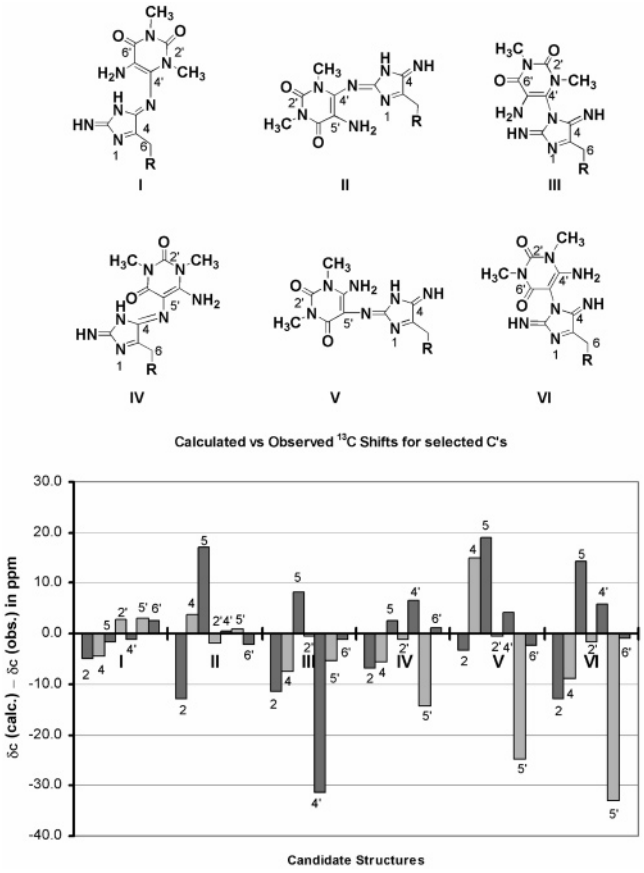

Figure 2. Evaluation of the six possible working structures of leucosolenamine (**5**) via ^{13}C chemical shifts. The carbon numbers are listed above each bar. R = benzo-1,3-dioxole moiety.

protons of substructure **B**. The only NOE correlations observed were from H-6 (δ_H 4.05) to H-8 (δ_H 6.97) and H-12 (δ_H 6.79) and vice versa.

We next turned to analyzing the ^{13}C chemical shifts expected for these possibilities and focused on three observed signals, at δ 113, 146, and 148, that appeared to be distinctive. The calculated ^{13}C chemical shifts (ACD software) versus experimental data are shown in Figure 2 (and Figure S9), and agreement of these data within ±5 ppm was considered to be diagnostic. The three key observations were as follows: (a) only structures **I**, **II**, and **III** showed good agreement for the data at C-5′, (b) the data set at C-4/C-4′ showed agreement for structures **I** and **II**, and not **III** or **V**, and (c) the data set at C-5 and C-2 showed the best agreement for structure **I**. Thus **I** emerged as the most consistent candidate, as shown by the excellent agreement of the δ_{C-calc} to δ_{C-obsv} and was confidently concluded to be the final structure of **5** (Figure 2). As seen here, employing database software to calculate ^{13}C shifts is becoming an invaluable tool to confirm structural assignments.[18]

To further substantiate the above conclusion, **5** was subjected to MS−MS in both positive and negative ion modes. The negative ion experiment gave an *m*/*z* 382.17 $[M - H]^-$, and further MS−MS on this ion produced a single fragment at *m*/*z* 340.01 corresponding to a loss of CN_2H_2, as shown in Figure 3. MS−MS on *m*/*z* of 340.01 resulted in a fragment ion of *m*/*z* 312.17 from a loss of CO. The direct loss of CN_2H_2 was not compatible with structure **III** or **VI** due to differences in regiochemistry, leaving two remaining possible mechanisms to explain these results. We preferred fragmentation pathway A beginning with **I** or **IV** involving two C−N bond cleavages at N-1−C-2 and N-3−C-4. As explained below, pathway B was less favored and resulted from a C−C bond cleavage occurring from **II** or **V** at the C-4−C-5 and C-2−N-3 bonds. Additional observations supporting pathway A were obtained by MS−MS on *N*,*N*-dimethylnaamidine D (**8**, Figure S15) and leucettamine B (**2**, Figure S16). The MS−MS on the $[M + H]^+$ at *m*/*z* 352.33 for **8** resulted in a loss of an anisole moiety to give fragment *m*/*z* 244.14, and further MS−MS on this fragment afforded the peak at *m*/*z* 188.04 rationalized by a loss of $C_2N_2H_4$ and is consistent with a N-1−C-2 and N-3−C-4 cleavage, shown in Figure 3A. A similar cleavage process was observed when a leucettamine B (**2**) $[M - H]^-$ peak at *m*/*z* 244.09 was subjected to MS−MS, eventually affording the peak at *m*/*z* 159.00 from loss of $C_2N_2H_3$ also via N-1−C-2 and N-3−C-4 cleavage, shown in Figure 3A. The key observation here is that the MS−MS data of **2** and **8** failed to show the cleavage at the C-4−C-5 bond expected via pathway B (as illustrated in Figure S16B). Some additional observations from the MS−MS data were not diagnostic as follows. Additional MS−MS on *m*/*z* 340.01 for **5** gave a new ion at *m*/*z* 312.17 from loss of CO to structure **5ii**. Positive ion mode MS−MS analysis of **5** (Figure S17) also gave interesting results but similar to the preceding data did not differentiate between structures **I**, **II**, **IV**, and **V**.

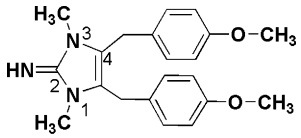

N,*N*-dimethyl naamidine D (**8**)

An especially critical step in evaluating the structure of **5** pertained to focusing on the major tautomer between the two possibilities shown in Figure 4. The NMR data of **5** clearly showed that only one major tautomer (structure **I** of Figure 2) was present, and this was concluded to be **5a** on the basis of the results of relative energies from MOPAC calculations and the best fit between observed and experimental ^{13}C shifts (Figure S18). Interestingly, the fully minimized structure of both tautomers (Figure S19) predicted that the phenyl ring and the pyrimidine ring should be positioned away from each other as shown and is consistent with the lack of NOE correlations between the proton-containing residues of these two rings.

We sought to extend the results obtained above by examining two additional PNG collections of this species. The two collections (nos. 05413 and 06123) were selected, and their crude extracts were combined and processed as described for collection no. 03528 (Figure S2). From the crude methanol extract six preparative HPLC fractions were obtained. Fraction 4 contained **5** (5.6 mg) and fraction 3 was further purified to give leucosolenamine B (**6**) (1.3 mg).

The structure elucidation of **6** began with obtaining a molecular formula from the HRESITOFMS $[M + H]^+$ *m*/*z* 397.1658, indicating $C_{18}H_{21}N_8O_3$ (Δ 7.0 mmu vs calc) and required 13 degrees of unsaturation. Comparing this formula to that of **5** showed a difference of $+C_1H_3N$ and −O, making it evident that one of the C═O in **5** was replaced by a C═NCH_3 group in **6**. Using the new NMR data in Table 2 for a side-by-side comparison with that of Table 1 indicated many structural similarities between the two compounds. The only differences in their ^{13}C NMR are an upfield shift of $\delta_{C-6'}$ in **6** at 145.3 versus $\delta_{C-6'}$ 159.5 in **5** plus there was an extra methyl signal at δ 38.1. From these NMR comparisons it was clear that **6** also contains a dioxybenzo-2-aminoimidazole and a 5,6-dinitrogen-substituted uracil moiety. These were confirmed by gHMBC correlations as illustrated in Figure 1, substructure **B**, and in Figure 5, substructure **D**. The important gHMBC correlations to fix the position of the C═NCH_3 are shown and were as follows. One set involved the correlation from methyl protons δ 3.55 and 3.22 to $\delta_{C-6'}$ 145.3, and the other set involved correlations from methyl protons δ 3.17 and 3.22 to $\delta_{C-2'}$ 150.8. The chemical shift of C-6′ is consistent with that observed in synthetic purinone derivatives with their *N*-methylimino carbons resonating at ~δ_C 144−147 (Figure S26).[19]

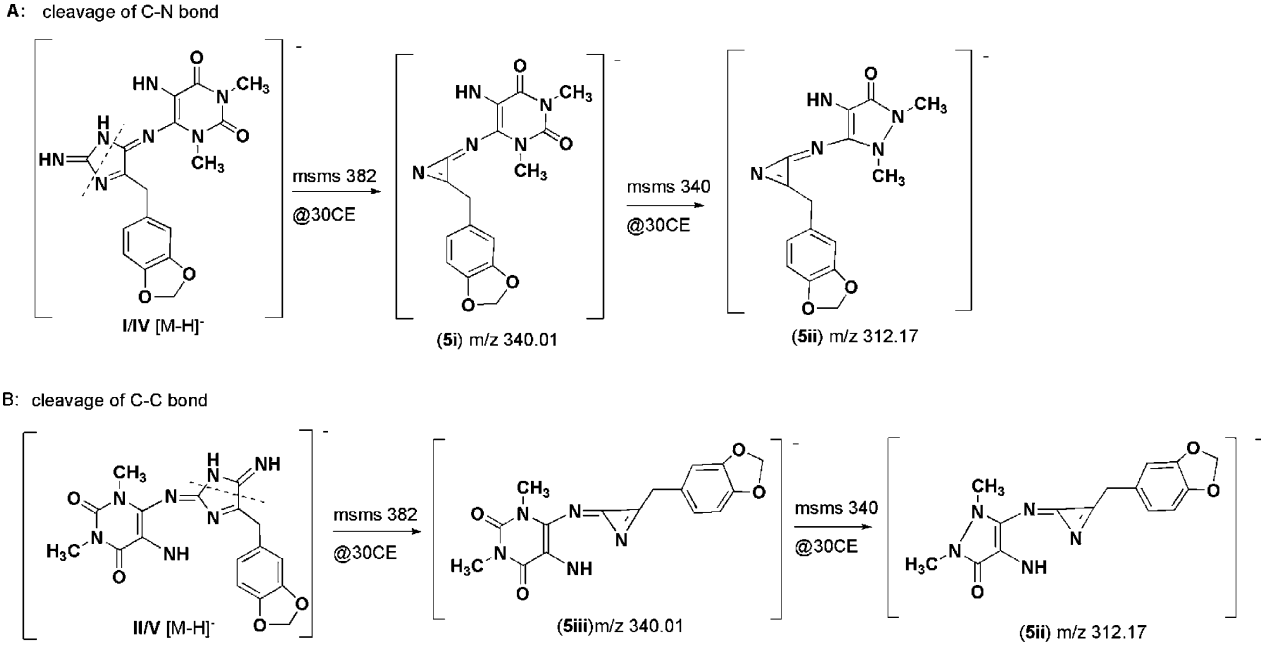

Figure 3. Proposed MS−MS fragmentation pattern of **5**. Pathway A rationalizes the fragmentation patterns for structures **I** and **IV**, while pathway B details the fragmentation patterns for **II** and **V**. See Figure 2 for candidate structures **I**, **II**, **IV**, and **V**. CE = collision energies set at 30 eV.

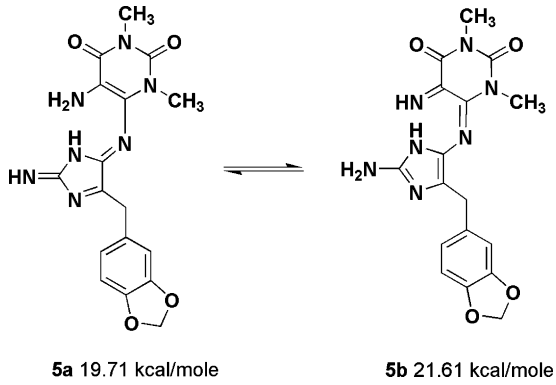

Figure 4. Relative energies of the two tautomeric forms of **5**.

Table 2. NMR Data of Leucosolenamine B (**6**) in DMSO-d_6 at 500 MHz (^{1}H) and 125 MHz (^{13}C)

C#	δ_C	δ_H mult. *J*(Hz), int.	gHMBC
2	159.7		
4	144.3		
5	155.5		
6	38.2	4.01, s, 2H	4, 5, 7, 8, 12
7	133.6		
8	110.0	6.93, d, 2.5, 1H	9, 10, 12
9	146.8		
10	145.3		
11	107.9	6.75, d, 8.0, 1H	7, 9, 10, 12
12	122.1	6.80, dd, 8.0, 2.5, 1H	6, 7, 8, 11
13	100.6	5.91, s, 2H	9, 10
2′	150.8		
4′	143.8		
5′	115.4		
6′	145.3		
CH_3-*N*1′	29.9	3.22, s, 3H	2′, 6′
CH_3-*N*3′	28.7	3.17, s, 3H	2′, 4′
CH_3-*N*6′	38.1	3.55, s, 3H	6′

Substructures **B** and **D** were then combined on the basis of parallel ^{13}C chemical shifts and biogenetic comparison to **5** to give the final structure of **6**. The analysis according to the strategy of Figure 4 (Figure S18) supported the tautomer shown. Last, a ROESY experiment on **6** showed only correlations from H-6 (δ_H 4.01) to H-8 (δ_H 6.39) and H-12 (δ_H 6.80), while no correlations were observed between the three *N*-Me protons of substructure **D** or from these protons to those of substructure **B**. From these observations, it was concluded that CH_3-*N*6′ is *trans* to CH_3-*N*1′, as shown in the final structure of **6**, and that the phenyl ring and the pyrimidine ring should be positioned away from each other as discussed above for **5**.

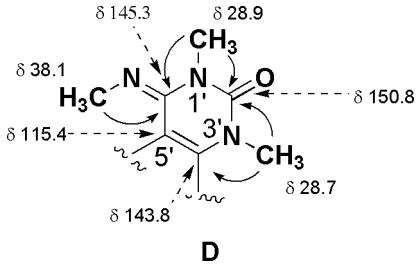

Figure 5. Substructure **D** showing ^{13}C chemical shifts and gHMBC correlations.

Table 3. Zone Unit Differentials in the Disk Diffusion Soft Agar Colony-Forming Assay[a]

compound	conc, μ**g**/disk	$Z_{C-38} - Z_{CFU-GM}$/mm
bengamide E (standard)	7.8	4.5
crude MeOH extract	180	9
5	180	10.5
XFMP1	180	16.5
7	180	0

[a] Murine cell lines: C-38, colon adenocarcinoma; CFU-GM, colony-forming unit-granulocyte macrophage; normal hematopoietic. Significant selectivity is defined by a difference of ≥7.5 mm zone unit differentials. XFMP1 is semipure and contains thymidine.

Our investigation of the biological properties was restricted to an evaluation of **5** due to sample limitation and stability. The data set summarized in Table 3 employed our standard disk diffusion assay[14] and revealed that **5**, at 180 μg/disk, inhibited murine C-38 cells with a 10.5 mm zone as compared to 0 mm against CFU-GM cells. This is the profile for a mildly potent selective cytotoxin when compared to the in vivo active agent bengamide E,[20] displaying at 7.8 μg/disk inhibition zones of 21 mm against C-38 and 16.5 mm against CFU-GM cells. A similar pattern was observed for a

semipure fraction (coded XFMP1) that yielded thymidine (**7**), and it showed a zone of inhibition of 21 mm against C-38 cells versus 4.5 mm against CFU-GM at 180 μg/disk. However, pure **7** was inactive when reassayed against C-38 and CFU-GM cells. Unfortunately, it has not been possible to date to isolate the active component of this semipure fraction.

The overall structures of leucosolenamines A (**5**) and B (**6**) while not overly complex are unprecedented and presented an extreme challenge to characterize. Their core structure retains the 2-amino imidazole array observed in other calcareous sponges. The substitution of *N*,*N*-dimethyl-5,6-diaminopyrimidine-2,4-dione and 5,6-diamino-1,3-dimethyl-4-(methylimino)-3,4-dihydropyrimidin-2(1*H*)-one at C-4 is unique and represents a new structural theme in calcareous imidazole alkaloid chemistry. Substructure **C** has been observed as a natural product in 1,3-dimethyl-4,5-diamino-2,6-dihydroxypyrimidine from an *Aspergillus nidulans*[21] and in hymeniacidin from a marine *Hymeniacidon* sponge.[22] Of additional note, this substructure is embedded in the pteridine ring of leucettidine (**9**), isolated from a Bermuda collection of *Leucetta microraphis*.[23] The discovery of **5** and **6** from *Leucosolenia* represents the first natural products from this genus and provides a stimulus to explore the other unstudied orders of the class Calcarea.

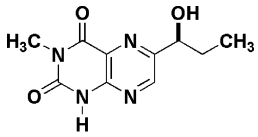

leucettidine (**9**)

Experimental Section

General Experimental Procedures. NMR spectra were obtained using a Varian Unity 500+ at 500 MHz for ^{1}H and 125 MHz for ^{13}C employing internal standards: DMSO-d_6 at δ_H 2.50 and δ_C 39.57. Multiplicities of ^{13}C NMR peaks were determined using DEPT and gHMQC data. ^{13}C NMR data of **6** were measured using a direct detection ^{13}C nano probe. Low- and high-resolution mass spectrometry was performed on a benchtop Mariner electrospray ionization time-of-flight instrument (ESITOF). Ultrahigh-resolution mass measurements were obtained via positive mode on a Finnigan FTICR hybrid mass spectrometer, which combines ion trap and Fourier transform ion cyclotron resonance.[15] MS−MS measurements were done using a LTQ mass spectrometer. Preparative HPLC was carried out using a single-wavelength (λ = 254 nm) UV detector and evaporative light-scattering detector (ELSD) in series with a Waters RP C18, 5 μm particle column. Computer modeling and calculations were done using ACD/^{13}C NMR DB version 8.00 (May 4th, 2005).

Biological Material. The sponge samples (UCSC coll. nos. 03528, 05413, 06123) were collected by scuba from a variety of sites off Milne Bay in Papua New Guinea at depths of 30−70 ft. The sponge was identified by Prof. Rob van Soest as a *Leucosolenia* sp., and a voucher sample has been deposited at the Zoological Museum of Amsterdam (ZMAPOR 17556). Voucher specimens and underwater photos are available from the author (P.C.).

Isolation. The sponge samples were preserved in the field according to our standard procedure and transported back to the laboratory at ambient temperature.[24] The preserved sponge (03528−1.06 kg, wet weight) was thoroughly dried, ground, and extracted with the accelerated solvent extractor (ASE) first with hexanes, next with CH_2Cl_2, and last with MeOH under high pressure (1700 psi) at 110 °C (Figure S2).[25] The MeOH extract was evaporated in vacuo to produce a brown, viscous oil. This oil was then subjected to preparative reversed-phase (RP) HPLC using a Waters C18, 5 μm particle column to afford five fractions. Fraction 3, which was the major metabolite, was eluted at 60% CH_3CN/H_2O to yield **5** (9.0 mg). Fraction 1 was also further purified by HPLC to yield **7** (12.2 mg).

Dried sponge samples (collections numbers 05413 and 06123, 1.31 kg wet weight) were extracted using the ASE employing the procedure outlined above (Figure S2). The MeOH-soluble fraction labeled XFM was subjected to preparative RP HPLC using 10−100% CH_3CN/H_2O to afford six fractions. Fraction 4 contained **5** (5.6 mg) while fraction 3 was further purified by semipreparative RP HPLC at 40% CH_3CN/H_2O to yield **6** (1.3 mg).

Leucosolenamine A (5): 9.2 mg, brown solid; ^{1}H NMR (DMSO-d_6, 500 MHz) and ^{13}C NMR (DMSO-d_6, 125 MHz), see Table 1 and Supporting Information; ^{1}H NMR of **5** was also taken in MeOH-d_4, acetone-d_6, dioxane-d_8, and THF-d_6 with and without TFA but no *N*H's were observed. NOESY correlations were observed from H-6 (δ_H 4.05) to H-8 (δ_H 6.97) and H-12 (δ_H 6.79) and vice versa; HRFTICRMS $[M + H]^+$ obsd 384.14161 (Δ0.04 mmu vs calc), calcd for $C_{17}H_{18}N_7O_4$ 384.14165. Hydrogenolysis of **5** was unsuccessful.

Leucosolenamine B (6): 1.3 mg, brown solid; ^{1}H NMR (DMSO-d_6, 500 MHz) and ^{13}C NMR (DMSO-d_6, 125 MHz), see Table 2 and Supporting Information; ROESY correlations observed were from H-6 (δ_H 4.01) to H-8 (δ_H 6.39) and H-12 (δ_H 6.80) and vice versa; HRESITOFMS $[M + H]^+$ obsd 397.1628 (Δ7.0 mmu vs calc), calcd for $C_{18}H_{21}N_8O_3$ 397.17311.

Thymidine (7): 12.2 mg, white needles; $[\alpha]_D$ +78.0 (*c* 0.61, H_2O); ^{1}H NMR (MeOH-d_4, 500 MHz) and ^{13}C NMR (MeOH-d_4, 125 MHz), see Supporting Information; HRESITOFMS $[M + H]^+$ obsd 243.10319 (Δ5.6 mmu vs calc), calcd for $C_{10}H_{15}N_2O_5$ 243.09755.

Acknowledgment. Financial support for this research was from NIH grant CA 47135. Prof. Rob van Soest of the University of Amsterdam provided the taxonomic identification of the sponge. Jack Cunniff of Thermo Electron Corporation provided the ultrahigh-resolution FTMS data. We also thank the captain and the crew of the *M/V Telita.* Special thanks are extended to L. Matainaho of the University of Papua New Guinea for assistance in collection permits.

Supporting Information Available: Compound isolation schemes, underwater and above water photographs of *Leucosolenia* sp., NMR spectra (^{1}H, ^{13}C NMR, gHMBC, gHMQC, DEPT) and MS spectra of **5**, **6**, and **7**, ACD calculations and MOPAC-minimized structures of **5a** and **5b**, MS−MS data of **2**, **5**, and **8**. This material is available free of charge via the Internet at http://pubs.acs.org.

References and Notes

(1) Blunt, J. W.; Copp, B. R.; Munro, M. H. G.; Northcote, P. T.; Prinsep, M. R. *Nat. Prod. Rep.* **2005**, *22*, 15−61.

(2) (a) Simmons, T. L.; Andrianasolo, E.; McPhail, K.; Flatt, P.; Gerwick, W. H. *Mol. Cancer Ther.* **2005**, *4*, 333−342. (b) Newman, D. J.; Cragg, G. M. *J. Nat. Prod.* **2004**, *67*, 1216−1238. (c) Crews, P.; Gerwick, W.; Schmitz, F.; France, D.; Bair, K.; Wright, A.; Hallock, Y. *Pharm. Biol.* **2003**, *41*, 39−52.

(3) (a) Thale, Z.; Kinder, F. R.; Bair, K. W.; Bontempo, J.; Czuchta, A. M.; Versace, R. W.; Phillips, P. E.; Sanders, M. L.; Wattanasin, S.; Crews, P. *J. Org. Chem.* **2001**, *66*, 1733−1741. (b) Kinder, F. R., Jr.; Versace, R. W.; Bair, K. W.; Bontempo, J. M.; Cesarz, D.; Chen, S.; Crews, P.; Czuchta, A. M.; Jagoe, C. T.; Mou, Y.; Nemzek, R.; Phillips, P. E.; Tran, L. D.; Wang, R.; Weltchek, S.; Zabludoff, S. *J. Med. Chem.* **2001**, *44*, 3692−3699.

(4) (a) Mooberry, S. L.; Randall-Hlubek, D. A.; Leal, R. M.; Hegde, S. G.; Hubbard, R. D.; Zhang, L.; Wender, P. A. *Proc. Natl. Acad. Sci. U.S.A.* **2004**, *101*, 8803−8808. (b) Quiňoa, E.; Kakou, Y.; Crews, P. *J. Org. Chem.* **1988**, *53*, 3642−3644.

(5) (a) Umera, D.; Takahashi, K.; Yamamoto, T. *J. Am. Chem. Soc.* **1985**, *107*, 4796−4798. (b) Bai, R. L.; Paul, K. D.; Herald, C. L.; Maspeis, L.; Pettit, G. R.; Hamel, E. *J. Biol. Chem.* **1991**, *266*, 15882−15889. (c) Dabydeen, D.; Florence, G.; Patterson, I.; Hanel, E. *Cancer Chemother. Pharmacol.* **2004**, *53*, 397−403. (d) Kuznetsov, G.; Towle, M. J.; Cheng, H.; Kawamura, T.; TenDyke, K.; Liu, D.; Kishi, Y.; Yu, M. J.; Littlefield, B. A. *Cancer Res.* **2004**, *64*, 5760−5766.

(6) (a) Gunasekera, S. P.; Gunasekera, M.; Longley, R. E.; Schulte, G. K. *J. Org. Chem.* **1990**, *55*, 4912−15. (b) Honore, S.; Kamath, K.; Braguer, D.; Horwitz, S. B.; Wilson, L.; Briand, C.; Jordan, M. A. *Cancer Res.* **2004**, *64*, 4957−4964.

(7) Piña, I. C.; Gautschi, J. T.; Wang, G.; Sanders, M. L.; Schmitz, F. J.; France, D.; Cornell-Kennon, S.; Sambucetti, L. C.; Remiszewski, S. W.; Perez, L. B.; Bair, K. W.; Crews, P. *J. Org. Chem.* **2003**, *68*, 3866−3873.

(8) (a) Crews, P.; Clark, D. P.; Tenney, K. *J. Nat. Prod.* **2003**, *66*, 177−182. (b) Ralifo, P.; Crews, P. *J. Org. Chem.* **2004**, *69*, 9025−9029. (c) Edrada, R. A.; Stessman, C.; Crews, P. *J. Nat. Prod.* **2003**, *66*, 939−942.

(9) (a) Ciminiello, P.; Fattorusso, E.; Magno, S.; Mangoni, A. *Tetrahedron* **1989**, *45*, 3873−3878. (b) Ciminiello, P.; Fattorusso, E.; Magno, S.; Mangoni, A.; Di Blasio, B.; Pavone, V. *Tetrahedron* **1990**, *46*, 4387−4392. (c) Hassan, W.; Edrada, R.; Ebel, R.; Wray, V.; Berg, A.; Van Soest, R.; Wiryowidagdo, S.; Proksch, P. *J. Nat. Prod.* **2004**, *67*, 817−822.

(10) Fu, X.; Schmitz, F. J.; Tanner, R. S.; Kelly-Borges, M. *J. Nat. Prod.* **1998**, *61*, 384−386.
(11) Chan, G. W.; Mong, S.; Hemling, M. E.; Freyer, A. J.; Offen, P. H.; DeBrosse, C. W.; Sarau, H. M.; Westly, J. W. *J. Nat. Prod.* **1993**, *56*, 116−121.
(12) Akee, R. K.; Carroll, T. R.; Yoshida, W. Y.; Scheuer, P. J.; Stout, T.; Clardy, J. *J. Org. Chem.* **1990**, *55*, 1944−1946.
(13) Hooper, J. N. A.; van Soest, R. W. M. *Systema Porifera. A Guide to the Classification of Sponges*; Kluwer Academic/Plenum Publishers: New York, 2002; Vol. 2, pp 1159−1161.
(14) Bioassay procedures are described in: Valeriote, F.; Grieshaber, C. K.; Media, J.; Pietraszkewicz, H.; Hoffmann, J.; Pan, M.; McLaughlin, S. *J. Exp. Ther. Oncol.* **2002**, *2*, 228−236.
(15) (a) Henry, K. D.; Williams, E. R.; Wang, B. H.; McLafferty, F. W.; Shabanowitz, J.; Hunt, D. F. *Proc. Natl. Acad. Sci. U.S.A.* **1989**, *86*, 9075−9078. (b) Zhang, L. K.; Rempel, D.; Pramanik, B. N.; Gross, M. L. *Mass Spec. Rev.* **2005**, *24*, 286−309.
(16) Carmely, S.; Ilan, M.; Kashman, Y. *Tetrahedron* **1989**, *45*, 2193−2200.
(17) Akee, R. K.; Carroll, T. R.; Yoshida, W. Y.; Scheuer, P. J.; Stout, T.; Clardy, J. *J. Org. Chem.* **1990**, *55*, 1944−1946.
(18) Rychonsky, S. D. *Org. Lett.* **2006**, *8*, 2895−2898.
(19) (a) Kozai, S.; Ogimoto, K.; Maruyama, T. *Tetrahedron* **2000**, *56*, 1685−769. (b) Müller, C. E.; Thorand, M.; Qurishi, R.; Diekmann, M.; Jacobson, K.; Padget, W. L.; Daly, J. *J. Med. Chem.* **2002**, *45*, 3440−3450.
(20) Segraves, N. L.; Robinson, S. J.; Garcia, D.; Said, S. A.; Fu, X.; Schmitz, F. J.; Pietraszkiewicz, H.; Valeriote, F. A.; Crews, P. *J. Nat. Prod.* **2004**, *67*, 783−792.
(21) Sadique, J.; Shanmugasundaram, R.; Shanmugasundaram, E. R. *Naturwissenschaften* **1966**, *53*, 282−286.
(22) Capon, R. J.; Skene, C.; Vuong, D.; Lacey, E.; Gill, J. H.; Heiland, K.; Friedel, T. *J. Nat. Prod.* **2002**, *65*, 368−370.
(23) Cardellina, J. H.; Menwald, J. *J. Org. Chem.* **1981**, *46*, 4782−4784.
(24) Jaspars, M.; Rali, T.; Laney, M.; Schatzman, R. C.; Diaz, M. C.; Schmitzs, F. J.; Pordesimo, E. O.; Crews, P. *Tetrahedron* **1994**, *50*, 7367−7373.
(25) A side-by-side comparison of sponge samples extracted using the ASE and successive soaking in solvent produced crude oils containing identical chemical profiles by LCMS. In addition, we have isolated the bengamides and the jasplakinolides using the ASE. Advantages of using the ASE include higher yields and low consumption of solvents.

NP060462B